Colorimetric Characterization of a Desktop Drum Scanner via Image Modeling

Roy S. Berns and M. J. Shyu
Munsell Color Science Laboratory, Center for Imaging Science
Rochester Institute of Technology, Rochester, New York

Abstract

A desktop scanner was colorimetrically characterized to average CIELAB error of less than unity for Kodak Ektachrome transparencies and Ektacolor paper, and Fuji Photo Film Fujichrome transparencies and Fujicolor paper. Independent verification on spectrally similar materials yielded average ΔE^*_{ab} error of less than 2.1. The technique first modeled the image formation of each medium using either Beer-Bouguer or Kubelka-Munk theories. Scanner digital values were then empirically related to dye concentrations. From these estimated dye concentrations, either spectral transmittance or spectral reflectance factor was calculated from an a priori spectral analysis of each medium. The spectral estimates can be used to calculate tristimulus values for any illuminant and observer of interest.

Introduction

It is hypothesized that colorimetric descriptions of images as input to desktop publishing and traditional photomechanical printing will improve color accuracy and reduce prepress time. Accordingly, four general methods have been described to transform digital image scanners to approximations of imaging colorimeters. The first method is to design the scanner as a colorimeter, e.g., references 1 and 2. Care must be taken to insure a sufficient number of quantization levels and dynamic range. The second method is to transform the scanner signal values to colorimetric data using a combination of one-dimensional functions or splines for gray balance and tone reproduction and a 3 by *n* color-correction matrix where *n* often varies from 3 to 64, e.g., references 3 and 4. The third method is to uniformly sample the scanner input space and build a look-up table; through multidimensional linear interpolation, colorimetric values are estimated[5, 6]. These three methods all ignore metamerism and as a consequence are constrained to a single medium, illuminant, and observer.

A spectral scanner would alleviate metameric problems; from a colorimetric perspective, developing such a device would have high priority. However, the engineering hurdles are formidable and as a consequence, commercial products are as yet, unavailable. A similar problem was encountered many years ago by the photographic industry. For certain aspects of film building, spectral data are required, ideally in various locations on an image. This was difficult to obtain because of the large aperture of most spectrophotometers and the slow speed of data collection. From a knowledge of the relationship between the amount of dye in the image area and its corresponding spectrum, one could use a densitometer to measure the dye amounts directly, and through a series of calculations, estimate the spectral values. This is known as the conversion from integral to analytical density[7]. This approach can be applied to the present problem since most scanners have spectral responsivities similar to status density responses[8-10]. A similar approach was used in this research to estimate either spectral transmittance or reflectance factor from scanner data for four photographic materials: Eastman Kodak Ektachrome and Ektacolor, and Fuji Photo Film Fujichrome and Fujicolor. Greater detail can be found in reference 11. The description of our methodology will be limited to Ektachrome.

Experimental

An Ektachrome ANSI IT8.7/1 target[12] was used to model the film's spectral characteristics and relate the scanner signals to dye concentrations. An independent target to test our methodology was produced by exposing 4" × 5" film using a digital film recorder and processing in the usual manner. This target was a digital 6×6×6 factorial design sampling the film's color gamut. The spectral transmittances of both targets were measured at the central 50% of each color patch using a Photo Research 703A spectroradiometer and constant-current daylight filtered tungsten-halogen lamp configured to achieve 0/0 geometry.

Targets were scanned on a Howtek D4000 drum scanner at 500 dots per inch. Data were collected at 12 bit quantization depth with a linear photometric response. The central 2500 pixels of each color patch were averaged forming the scanner data base. The independent target was scanned on a different day from the modeling target.

Color Formation Theory of Transparent Photographic Media

Photographic positive film following processing can be considered, first order, as a transparent medium consisting of dyed gelatin. The three dyes, cyan, magenta, and yellow, are assumed to not scatter light, not fluoresce, and not affect the refractive index of the medium. Following these assumptions, the relationship between the amount of dye in the film and spectral transmittance can been described by the Beer-Bouguer theory:

$$T_\lambda / T_{\lambda,\max} = e^{-(c_c D_{\lambda,c} + c_m D_{\lambda,m} + c_y D_{\lambda,y})} \quad (1)$$

where c_c, c_m, and c_y are the concentrations, $D_{\lambda,c}$, $D_{\lambda,,m}$, and $D_{\lambda,y}$ are the unit spectral absorptivities of cyan, magenta, and yellow, respectively, $T_{\lambda,\max}$ is the maximum spectral transmittance of the entire target, and T_λ is the spectral transmittance of a given color patch. The units of concentration can be by weight, volume, or relative to a nominal exposure (similar to equivalent neutral densities). The latter method was used. Once T_λ is known, tristimulus values are calculated. For this research, CIE illuminant D50 and the 1931 standard observer were used as specified by ANSI,[13] although any illuminant and observer can be used.

Estimating Dye Absorptivity Spectra

Eigenvector analysis was performed[14] (covariance form with equimax rotation) using the spectral absorption data of all the patches of the IT8.7/1 target where absorption was calculated as

$$D_\lambda = - \ln(T_\lambda / T_{\lambda,max}) \quad (2)$$

The first three eigenvectors accounted for 99.96% of the population variance providing an excellent description of the spectral properties of the film. One limitation of these vectors was a lack of spectral similarity to real dyes. We hypothesized that if nonlinear transformations were required to relate dye concentration and digital counts, better performance would result if the eigenvectors were rotated to resemble actual dyes. Because we do not have access to single-dye coatings and it is nearly impossible to have only a single developed dye due to inter-image effects, we performed three additional sequential eigenvector analyses on the cyan, magenta, and yellow ramps (columns 13-15 of the target), respectively, where it was assumed that the first eigenvector of each analysis would represent a single dye. These dyes were used as aim spectra in the rotation. The two sets of eigenvectors are shown in figure 1. The small lack of spectral similarity was expected and is often referred to as "Beer's law failure." The theoretical assumptions associated with Beer-Bouguer theory are not perfectly met in practice.

Estimating Dye Concentration

Viggiano and Wang[10] used the scalars from the eigenvector analysis as an estimate of the dye concentrations. This corresponds to a spectral match minimizing sum of squares spectral error. Dunne[8] and Rodriguez and Stockham[9] minimized integral density differences between the measured scanner values and their estimate based on a knowledge of the scanner's spectral properties (detector responsivity, optics, source) and the film's spectral transmittance. This corresponds to a densitometric match minimizing sum of squares density error. If the photographic medium is perfectly modelled using Beer-Bouguer theory, the two methods would yield identical results when using the same dye absorptivities. As described above, there is a small amount of Beer's law failure. As a consequence, a tristimulus matching algorithm was used to estimate dye concentrations[15, 16]. This method is described in detail by Berns[17] who applied this technique to a dye-diffusion thermal transfer printer. Tristimulus matches were obtained for illuminant D50 and the 1931 standard observer.

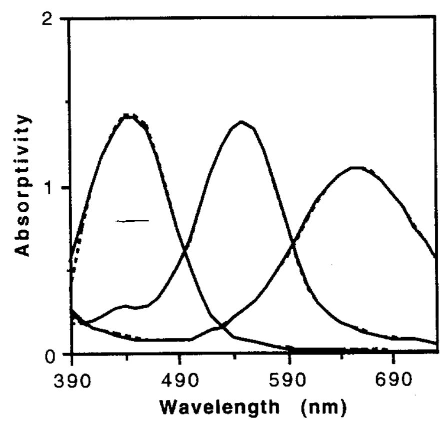

Figure 1. Dye absorptivities of Ektachrome. Rotated eigenvectors are shown by the solid lines; three sequential first eigenvectors are shown by the dashed lines.

The extent of "Beer's law failure" can be shown by calculating color differences for an illuminant dissimilar to D50 such as illuminant A. This is an index of metamerism. For this film, the average color difference was 0.2 ΔE*ab with a maximum of 0.5; the histogram is shown in figure 2. This amount of error could occur in the methods used by Dunne, Rodriguez, and Viggiano.

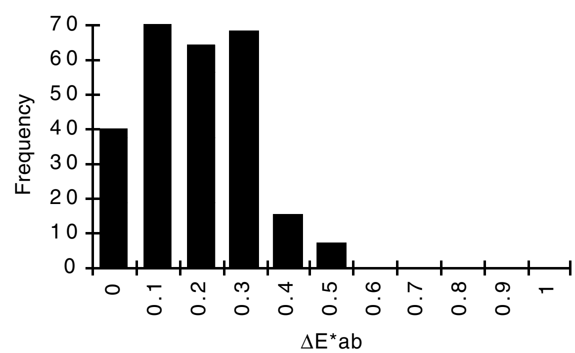

Figure 2. Color difference histogram for illuminant A quantifying degree of Beer's law failure.

Relating Scanner Data to Dye Concentration

From the Beer-Bouguer theory, a logarithmic response was expected. Following a natural logarithmic transformation, small nonlinearites remained that were modeled by stepwise polynomial regression (forward selection, $\alpha = 0.05$). The neutral step wedge was used for this analysis and thus modeled the tone reproduction and gray balance characteristics of the scanner and target. The equation for the red channel (d_r) was:

$$D_r = -0.27423 + 0.85435\,(\ln(d_r / (2^{12} - 1))) + 0.00004\,(\ln(d_r / (2^{12} - 1)))^5 \qquad (3)$$

If the scanner's spectral responsivities are similar to delta functions, a 3 × 3 transformation following the tone reproduction characterization will accurately predict dye concentrations. However, the scanner's responses are on the order of 50 nm wide at half height and asymmetrical. Because integrating logarithmic data is not equivalent to applying a logarithm on integrated linear data, a second nonlinear relationship was expected despite the above nonlinear transformation. Stepwise multiple linear regression (forward selection, $\alpha = 0.05$) was performed where the gray balanced values were the independent data and the actual concentrations were the dependent data. Linear, squared, and linear covariance terms were hypothesized as candidate model coefficients. For example, the relationship between gray-balanced values and cyan concentration (c_c) was as follows:

$$c_c = -0.027 + 1.427D_r - 0.565D_g + 0.068D_b - 0.085D_rD_g + 0.037D_r^2 + 0.051D_g^2 - 0.008D_b^2 \qquad (4)$$

The predicted concentrations were used to calculate spectral transmittance using equation (1), and in turn, tristimulus values.

Results and Discussion

The ΔE^*_{ab} histogram for the Ektachrome target is shown in figure 3 where the predicted tristimulus values are compared with the measured tristimulus values. Summary statistics are listed in Table I. Because maintaining gray balance is critical for many images, the neutral scale was separately analyzed; it had an average ΔE^*_{ab} of 0.35 and an average ΔH^*_{ab} of 0.10. A C^*_{ab} vs. L^* vector plot is shown in figure 4 for the neutral scale. If the transformation equations maintain gray balance, the vectors would have zero length. A change in vector angle from vertical represents a change in tone reproduction. Gray balance and tone reproduction are maintained despite the global nature of the final regression.

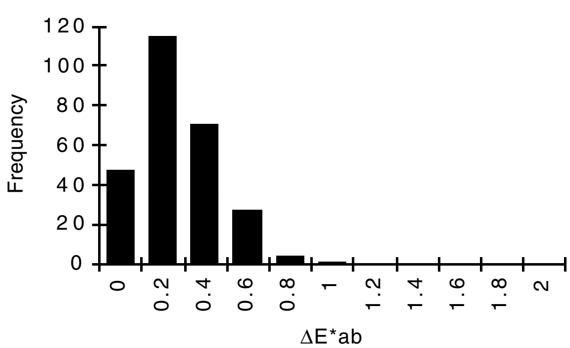

Figure 3. Color difference histogram for Ektachrome modeling IT8.7/1 target.

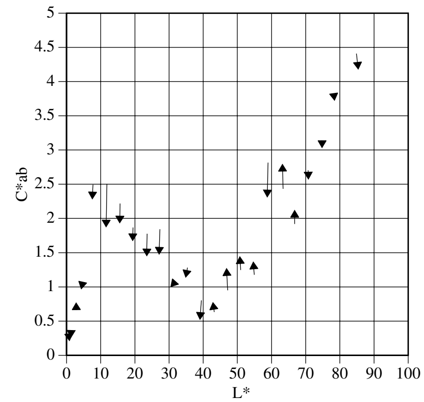

*Figure 4. C*ab vs. L* vector diagram of Ektachrome IT8.7/1 neutral scale. Vector tail locates measured value; vector head locates predicted value.*

Most of the previously published results have only provided model data results. Polynomial regression is very susceptible to poor performance in practice, a result of fitting random error in addition to the desired systematic trends. Direct table look up and interpolation is susceptible to measurement errors and quantization errors if the number of nodes is too small. Thus, independent verification is essential. The independent target was evaluated using the equations optimized for the IT8.7/1 target. If this method is robust, the color differences should be similar to the model data with these differences randomly distributed within the color gamut. The ΔE^*_{ab} histogram is shown in figure 5; mean and maximum values are listed in Table I. Although not shown, the color were mainly random in color space with a weak trend where color differences increased slightly with chroma (C^*_{ab}).

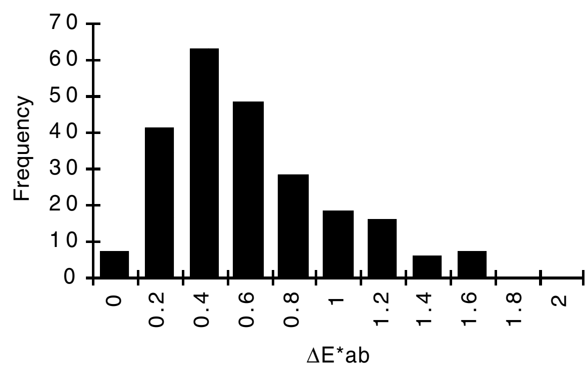

Figure 5. Color difference histogram of Ektachrome independent verification target.

Table I lists the results for the four films analyzed in this research. The 95th percentile was slightly greater than two times the mean of each data set. For example, 95% of the colors had a ΔE^*_{ab} less than 2 for the Ektacolor Q60C target. For the photographic papers, Kubelka-Munk theory was used to relate dye concentrations with spectral reflectance factor as described by Berns[17]. Also, the images were scanned at 8 bit quantization depth. This technique was very effective for positive films and slightly less effective for photographic

Table I. Summary Results

Material type	Ektachrome film	Fujichrome film	Ektacolor Plus paper	Fujicolor paper
Modeling target	Kodak IT8.7/1	Fuji IT8.7/1	Kodak Q-60C	Fuji IT8.7/2
Avg. ΔE^*_{ab} of modeling target	0.37	0.41	0.89	0.88
Max. ΔE^*_{ab} of modeling target	1.03	1.57	5.17	3.42
Avg. ΔE^*_{ab} of independent target	0.71	0.67	2.09	8.75
Max. ΔE^*_{ab} of independent target	1.78	1.56	7.29	21.30

papers. In the case of Ektacolor Plus paper, the empirical model relating linearized scanner values (Dr, Dg, Db) to dye concentration had greater residual error than the transparent materials; this was due to the wide-band scanner spectral sensitivities and quantization errors at high concentrations. For the Fujicolor paper, the independent data had large systematic errors. In a post hoc analysis, it was found that the independent target had different dye characteristics than the IT8.7/2 target; as a result, the spectral reconstruction was in error.

The results of Stokes, *et al.*[18,19] can be used as a goodness criterion where a perceptibility experiment was performed comparing perturbed images with an original image. Images with average errors less than about $2\Delta E^*_{ab}$ were indistinguishable. For Ektachrome, Fujichrome, and Ektacolor, the results are below the visual threshold when used for pictorial images. Presumably, the Fujicolor model would have equivalent performance to Ektacolor if the identical paper is used.

Conclusions

Applying the well-known technique of converting integral to analytical density to scanner colorimetric characterization yielded excellent results for transparency materials and very acceptable results for reflective materials. The key issues include characterizing the spectral absorptivity properties of the film, narrow-band scanner responsivities, and insuring the image requiring characterization has the same spectral absorptivity characteristics as the model data. This method has the advantage of easily characterizing the scanner for any illuminant and observer of interest, minimizing problems of metamerism. Its one limitation is that the film type must be known and been previously characterized.

Acknowledgments

This research was kindly supported by Dupont Printing and Publishing Division and Howtek.

References

1. P. G. Engeldrum, Color scanner colorimetric design requirements, *Proc. SPIE*, **1909**, 75-83 (1993).
2. M. J. Vrhel and H. J. Trussell, Filter considerations in color correction, *IEEE Trans. on Image Processing*, **3**, 147-161 (1994).
3. H. R. Kang, Color scanner calibration, *J. Imaging Sci. Tech.*, **36**, 162-170 (1992).
4. J. D. Clippeleer, Device independent color reproduction, *Proc. TAGA*, 98-106 (1993).
5. P. C. Hung, Colorimetric calibration in electronic imaging devices using a look-up-table model and interpolations, *J. Electronic Imaging* **2**, 53-61 (1993).
6. J. M. Kasson, W. Plouffe, S. I. Nin, A tetrahedral interpolation technique for color space conversion, *Proc. SPIE*, **1909**, 127-138 (1993).
7. P. Kowaliski, Sensitometry of color films and papers, in T. H. James, Ed., *The Theory of the Photographic Process*, 4th ed., MacMillan Publishing, New York, NY, 1977.
8. B. Dunne and T. G. Stockham, Method of converting scanner signals into colorimetric signals, U. S. Patent 5149960 (1992).
9. M. A. Rodriguez and T. G. Stockham, Producing colorimetric data from densitometric scans, *Proc. SPIE,* **1913**, (1993).
10. J. A. S. Viggiano and C. J. Wang, A novel method for colorimetric calibration of color digitizing scanner, *Proc. TAGA*, 143-160 (1993).
11. M. J. Shyu, Colorimetric characterization of a desktop drum scanner using spectral models, M.S. Thesis, Rochester Institute of Technology (1994).
12. D. McDowell, Summary of IT8/SC4 color activities, *Proc. SPIE,* **1913** (1993).
13. NPES the Association for Suppliers of Printing and Publishing Technologies, ANSI CGATS.5-1993 Graphic technology - Spectral Measurement and Colorimetric Computation for Graphic Arts Images, 1993.
14. L. Wilkinson, SYSTAT: The System for Statistics, Evanston, IL: SYSTAT, Inc., 1989.
15. N. Ohta, Fast computing of color matching by means of matrix representation, part I transmission-type colorant, *Appl. Opt.,* **10**, 2183-2187 (1971).
16. E. Allen, Colorant formulation and shading, in Eds. F. Grum and C. J. Bartleson, Eds., *Optical Radiation Measurement,* Vol. **2** *Color Measurement*, Academic Press, New York, 1980.
17. R. S. Berns, Spectral modeling of a dye diffusion thermal transfer printer, *J. Electronic Imaging,* **2**, 359-370 (1993).
18. M. Stokes, M. Fairchild and R. S. Berns, Colorimetrically quantified tolerances for pictorial images, *Proc. TAGA,* **2**, 757-778 (1992).
19. M. Stokes, M. Fairchild, and R. S. Berns, Precision requirements for digital color reproduction, *ACM Transactions on Graphics,* **11**, 406-422 (1992).